Pis'ma v ZhETF, vol. 96, iss. 2, pp. 114 – 117

Direct observation of standing electron waves in diffusively conducting InAs nanowire

A. A. Zhukov[+], *Ch. Volk*[*×], *A. Winden*[*×], *H. Hardtdegen*[*×], *Th. Schäpers*[*×°]

[+]*Institute of Solid State Physics of the RAS, 142432 Chernogolovka, Russia*

[*]*Grünberg Institut (PGI-9), Forschungszentrum Jülich, 52425 Jülich, Germany*

[×]*JARA-Fundamentals of Future Information Technology, Forschungszentrum Jülich, 52425 Jülich, Germany*

[°]*II. Physikalisches Institut, RWTH Aachen University, 52056 Aachen, Germany*

Submitted 20 June 2012

We investigate the disturbance of the InAs nanowire resistance by a conductive tip of a scanning probe microscope at helium temperature as a function of the tip position in close vicinity to the nanowire. At the tip displacement along the wire the resistance ($R_{\rm wire} \simeq 30\,{\rm k}\Omega$, what is typical for diffusive regime) demonstrates quasi-periodical oscillations with an amplitude about 3%. The period of the oscillations depends on the number of electrons in the nanowire and is consistent with expected for standing electron waves caused by ballistic electrons in the top subband of the InAs nanowire.

Inhomogeneous distributions of the electron density in metallic systems caused by peculiarities of electron wave function are well established in a number of different electron systems. Electron density waves in 2-dimensional electron gases [1] and Friedel oscillations in an Ag covered Si-surface [2] are popular examples of such inhomogeneous distributions. The typical scale of these oscillations is conventionally microscopic one, comparable with atomic scale. Below we report on the direct observation of standing electron waves in an InAs nanowire with a period between micro- and nanoscale. Moreover, such long range electron density oscillations are observed in the wire with formally diffusive conductivity.

The possibility to change the density of the electrons in nanowire by applying voltage to nearby placed electrode, a back gate for example, allows to realize nanowire-based field-effect transistors (FET). During the last decade substantial efforts have been made to investigate the electron transport in InAs nanowires [3–7]. In the *off-state* these transistors have resistances of several hundreds MΩ while in the *on-state* the resistance drops to 20–30 kΩ. Taking into account the possible application of InAs nanowire in electronics strong efforts were made to study the dependence of the mobility of the InAs nanowires on their diameter [6].

At low temperatures the transport in InAs wires is mostly diffusive. Transport measurements performed at He temperatures [3, 5] yielded typical values of the elastic mean free path l_e in the order of a few tenth of nanometers. In addition at low temperature phase-coherent transport was investigated, i.e. the temperature dependence of universal conductance fluctuations [4] and the suppression of weak antilocalization were investigated [3, 5]. In both cases a good agreement with theoretical predictions based on the dominance of diffusive transport was found. However, in contrast to the relatively small l_e values reported above, Zhou et al. [8] obtained considerably larger values exceeding 200 nm even at room temperature. So far, scanning gate microscopy (SGM) measurements conducted at $T = 4.2\,{\rm K}$ on InAs nanowire FETs have only been focused on electron transport in the regime close to pinch-off [10, 9]. Here, a number of peculiarities in Coulomb blockade regime were found.

In the current letter we report on SGM measurements in the open FET regime with relatively low nanowire resistance of $\sim 30\,{\rm k}\Omega$. Standing electron waves are observed in the SGM scans. It is found that the period of the standing electron waves depends on the number of electrons in the wire. We interpret the observation of the standing electron waves as an indication of the presence of ballistic electrons in InAs nanowire.

In our experiment we study a nominally undoped InAs nanowire grown by selective-area metal-organic vapor-phase epitaxy [11]. The diameter of the wire is 100 nm. The wire was placed on an n-type doped Si (100) substrate covered by a 100 nm thick SiO_2 insulating layer. The Si substrate served as the back-gate electrode. The evaporated Ti/Au contacts to the wire as well as the markers of the search pattern were defined by electron-beam lithography. The distance between the

contacts is $L_{\rm wire} = 2.6\,\mu$m. A scanning electron micrograph of the sample under investigation is shown in Fig. 1a. The source and drain metallic electrodes connected to the wire are marked by "s" and "d".

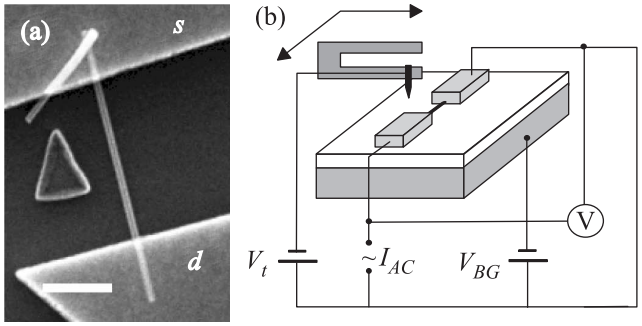

Fig. 1. (a) – Scanning electron micrograph of the InAs wire. The source and drain contact pads are marked by "s" and "d". The horizontal scale bar corresponds to $1\,\mu$m. The metallic triangle on the left side of the wire is a marker of the search pattern. (b) – Electrical circuit of the scanning gate microscopy measurements. The back-gate voltage V_{BG} is applied to the doped Si substrate while the tip voltage V_t is applied to the tungsten tip of the probe microscope. The resistance of the wire is measured using a two terminal circuit by applying a current (I_{AC}) and measuring the voltage (V). Further details are given in the main text

All measurements were performed at $T = 4.2$ K. The charged tip of a home-built scanning probe microscope [12] is used as a mobile gate during scanning gate imaging measurements. We keep the tip 300 nm above the SiO_2 surface, in order to eliminate any mechanical or electrical contact of the tip to the InAs wire or metallic contacts. All scanning gate measurements were performed by keeping the potential of the scanning probe microscope tip (V_t) and the back-gate voltage (V_{BG}) constant. The electrical circuit of the scanning gate imaging measurements is present in Fig. 1b. Details of the circuit can be found elsewhere [13].

The conductance of the wire during the scan is measured in a two-terminal circuit by using a standard lock-in technique. Here, a driving AC current with an amplitude of $I_{AC} = 1$ nA at a frequency of 231 Hz is applied while the voltage is measured by a voltage amplifier.

Figs. 2a–d present a set of the scanning gate measurements performed with a constant tip voltage of $V_t = 0$ V and a back-gate voltages of $V_{BG} = 11.8$, 10.6, 9.2, and 8.0 V, respectively. It can clearly be seen that the tip position strongly affects the wire resistance. The cross cuts of the SGM scans (Figs. 2a–d) along the wire are present in Figs. 2e–h. The cross-cut in Fig. 2h is obtained after subtracting of smooth background. With the displacement of the tip along the wire a quasi-periodic oscillation of the wire resistance with an amplitude of about 3% of the total resistance are observed. The period of these oscillations increase with decreasing back-gate voltage (Figs. 2a–c, e–g) until it abruptly becomes small again (Figs. 2d, h). As an example, 4, 3, and 2 equidistant minima in the nanowire resistance are marked by arrows in Fig. 2e–g, respectively. An abrupt change of the period is observed between the back-gate voltage 9.2 and 8 V. To make the period change visible we mark in Fig. 2h the equidistant maxima of resistance by arrows.

We argue that the periodic oscillations of wire resistance can be attributed to the presence of the standing electron waves in the nanowire. Let us consider the experimental situation in more details. The number of electrons in our wire at $V_{BG} = 10$ V is given by [7]:

$$N \sim \frac{(V_{BG} - V_{\rm pinch-off})\alpha \cdot 2\pi\varepsilon\varepsilon_0 L_{\rm wire}/e}{\ln\left[d_{ox} + r + \sqrt{(d_{ox}+r)^2 - r^2}\right)/r\right]} \sim 2300. \quad (1)$$

Here, $V_{\rm BG} - V_{\rm pinch-off} \sim 10$ V, $\alpha = C_{\rm wire-to-gate}/C_{\rm total} \sim 0.3$ is the ratio of wire to back-gate and total capacitance of the wire, $\varepsilon = 3.8$ is the SiO_2 permittivity, ε_0 is the permittivity of free space, $d_{\rm ox} = 100$ nm, and $r = 50$ nm are the thickness of the oxide layer and the wire radius, and e is elementary charge. Knowing the geometrical sizes of the wire it is possible to calculate the mean concentration of the electrons $n_{3D} \sim 1.1 \cdot 10^{17}\,{\rm cm}^{-3}$ [14]. The reciprocal radius of Fermi sphere calculated by considering the InAs nanowire as a 3D structure is $2\pi/k_{F,3D} = 2\pi/(3\pi^2 n_{3D})^{1/3} \sim 40$ nm, and the elastic mean free path in the wire is $l_e = \sqrt[3]{3/8\pi n_{3D}^2}(h/e^2)(1/R_{\rm wire})(L_{\rm wire}/\pi r^2) \sim 50$ nm, with h the Planck constant. Thus, the statement "InAs wire is a $3D$ structure in diffusive, close to the Ioffe–Regel limit regime $k_{\rm F,3D} l_e \sim 1$" mentioned previously looks quite reasonable. For these nominally undoped InAs nanowires the main source of scattering is surface scattering, due to irregularities caused by stacking faults or due to surface contaminations [14].

On the other hand, the evaluation of l_e seems to be too underestimated, because different electron groups in the wire have rather different mean free path. In an ideal one-dimensional wire there are a number of partially filled energy subbands due to the transverse quantization, as it is illustrated in Fig. 3. Because the conductance of the real nanowire is about e^2/h and the number of subbands is about 10–20, we have to conclude that the main part of electrons on Fermi level is in the diffusive regime. They are labeled as *disordered sea* in Fig. 3. Only electrons in the top one or two subbands below the Fermi level ($E_{\rm F}$) have a very large wavelength along the wire axis and, correspondingly, a small scattering probability at the smaller scale potential fluctuations caused

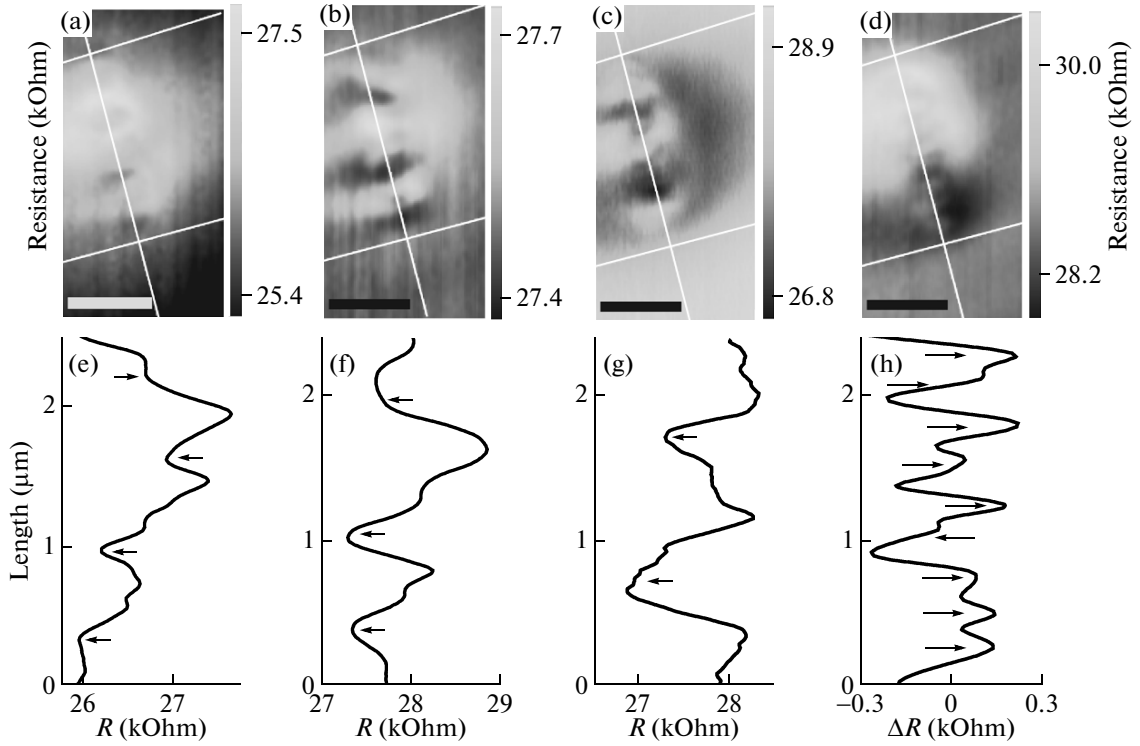

Fig. 2. (a)–(d) – SGM scans performed at $T = 4.2$ K with a constant tip voltage of $V_t = 0$ V and the back-gate voltages of $V_{BG} = 11.8$, 10.6, 9.2, and 8.0 V, respectively. The white lines denote the wire axis and the boundaries of source and drain electrodes. The orientation of the scans a–d is the same as in Fig. 1a. The horizontal scale bars in Figs. a–d correspond to 1 μm. (e)–(h) – Cross cuts of the SGM scans (Figs. a–d) made along the wire axis from the drain to the source electrodes. The cross cut in h was obtained after subtracting the smooth background

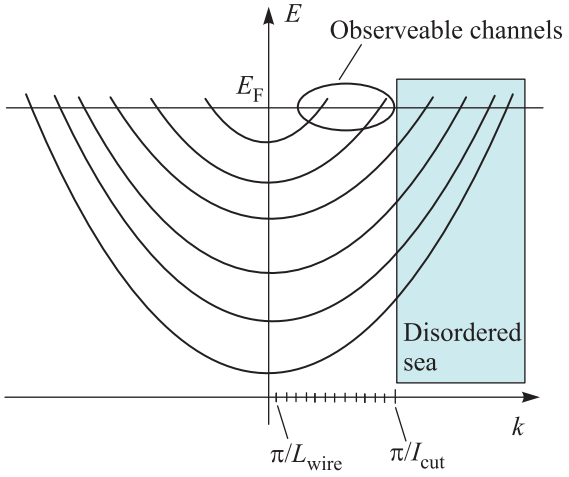

Fig. 3. Schematic band diagram of the InAs wire, here k is directed along the wire axis. Top subbands with small $k_F < \pi/l_{cut}$ form standing waves visualized in the SGM images, as can be seen in Fig. 2. The lower lying subbands with $k_F > \pi/l_{cut}$ form the "disordered sea", and no individual channels can be distinguish in this case

by the surface roughness. They have a wavelength $1/k_F$ comparable to the length of the wire (2.6 μm) and can form a standing electron wave due to the reflection from the contact barriers [9].

Lets focus on the alteration of the wavelength of standing electron wave with changing the back-gate voltage. With decreasing V_{BG} number of electrons and k_F of the top subband decrease. Thus, number of nodes or half waves must decrease either. Standing waves with 4, 3, and 2 nodes shown in Figs. 2a–c, e–g illustrate this trend. With further decreasing of back-gate voltage the top subband is depleted and the lower lying subband forms a multi-node standing wave (see Figs. 2d, h). Thus the depletion procedure of the top subband and formation of the ballistic channel with standing wave by lower lying subband is completed.

We do not observe standing waves with a wavelength less than $l_{cut} \sim 200$ nm. This is reasonable because the scattering rate for electrons with $k_F > \pi/l_{cut}$ nm must increase dramatically because 200 nm is close to the wire diameter of 100 nm, thus no individual channels may be distinguished. The zone with $k_F > \pi/l_{cut}$ is labeled in Fig. 3 as *disordered sea*. Additionally, the smallest tip to center of the wire distance is 250 nm. Taking into account the thickness of the SiO_2 layer ($d_{ox} = 100$ nm)

we can conclude that l_{cut} is quite close to the spatial resolution of our current experimental setup.

The exact mechanism of the influence of the ballistic electrons on the total conductance of the wire has not been clear by now. Additional experiments at different temperatures need to be done.

At first glance, we may attribute mechanism of the altering of the total resistance by standing waves to Fano resonances similar to the ones observed in carbon nanotubes [15] or in a one-lead quantum dot [16]. Electrons moving from source to drain may pass through a "disordered sea" (Path A) maintaining some information of their phases or path through a ballistic channel with a standing wave (Path B). Altering energy level of channel and muting it out of standing waves resonance with Coulomb potential created by charged tip [13] we alter mutual phases of the electrons passed through Path A and Path B [16]. If this mechanism is realized in the wire the decreasing of the temperature might result in a growing influence of the standing wave channel on the total resistance due to the increase of the phase coherence length [4].

In conclusion, we performed scanning gate microscopy measurements of an InAs quantum wire FET in the linear regime at high back-gate voltages when the resistance of the wire is of $30\,\text{k}\Omega$. Standing electron waves were observed in SGM scans. Their wavelength depends on the number of electrons in the wire. We attribute these standing waves to the presence of ballistic electrons in the top subband of the InAs nanowire.

We thank V.F. Gantmacher and V.T. Dolgopolov for useful discussions. This work is supported by the Russian Foundation for Basic Research, programs of the Russian Academy of Sciences, the Program for Support of Leading scientific Schools, and by the International Bureau of the German Federal Ministry of Education and Research within the project # RUS 09/052.

1. M. A. Topinka, B. J. LeRoy, R. M. Westervelt et al., Nature **410**, 183 (2001).
2. M. Ono, Y. Nishigata, T. Nishio et al., Phys. Rev. Lett. **96**, 016801 (2006).
3. P. Roulleau, T. Choi, S. Riedi et al., Phys. Rev. B **81**, 155449 (2010).
4. S. Estevez Hernandez, M. Akabori, K. Sladek et al., Phys. Rev. B **82**, 235303 (2010).
5. S. Dhara, H. S. Solanki, V. Singh et al., Phys. Rev. B **79**, 121311(R) (2009).
6. A. C. Ford, J. C. Ho, Yu-L. Chueh et al., Nano Lett. **9**, 360 (2009).
7. Sh. A. Dayeh, Semicond. Sci. Technol. **25**, 024004 (2010).
8. X. Zhou, S. A. Dayeh, D. Aplin et al., Appl. Phys. Lett. **89**, 053113 (2006).
9. A. A. Zhukov, Ch. Volk, A. Winden et al., Jetp. Lett. **93**, 13 (2011).
10. A. C. Bleszynski, F. A. Zwanenburg, R. M. Westervelt et al., Nano Lett. **7**, 2559 (2005).
11. M. Akabori, K. Sladek, H. Hardtdegen et al., J. Cryst. Growth **311**, 3813 (2009).
12. A. A. Zhukov, Instrum. Exp. Tech. **51**, 130 (2008).
13. A. A. Zhukov and G. Finkestein, JETP Lett. **89**, 212 (2009).
14. S. Wirths, K. Weis, A. Winden et al. J. Appl. Phys., **110**, 053709 (2011).
15. B. Babic and C. Schönenberger, Phys. Rev. B **70**, 195408 (2004); J. Kim, J.-R. Kim, J.-O. Lee et al., Phys. Rev. Lett. **90**, 166403 (2003).
16. A. C. Johnson, C. M. Marcus, M. P. Hanson, and A. C. Gossard, Phys. Rev. Lett. **93**, 106803 (2004).